BMC Musculoskeletal Disorders

RESEARCH

Open Access

The effects of mechanical stimulation on the morphology and function of spinal ligament cells

Tao Tang[1,2†], Fuan Wang[2†], Xizhe Liu[3†], Shaoyu Liu[2,3], Zhiyu Zhou[2,3*] and Lin Chen[4*]

Abstract

Background It has been shown that mechanical signaling in the cellular microenvironment is crucial for control at the cellular and tissue levels, affecting human growth and the prevalence of disease. Ligament cells from individuals with posterior longitudinal ligament ossification (OPLL) have been found to respond to external mechanical stimulation. However, the response of mechanical stimulation to OPLL ligament cells is unclear. This study aims to comprehensively assess the effects of mechanical stimulation on the proliferation, viability, shape and function of OPLL ligament cells.

Methods Eleven OPLL and 11 non-OPLL patient-derived Ligament cells were selected for this study. cells of test groups were exposed to 10% uniaxial cyclic stretch at frequency of 0.5 Hz for 3 h to 48 h. Calcein-AM/PI/Hoechst33342 assay was used to detect the activity of ligament cells. The CCK8 test was used to investigate the effect of stretch on cell proliferation. The level expression of pro-inflammatory factors was detected by using RT-qPCR. Cytoskeleton staining was used to evaluate changes in cytoskeleton morphology.

Results The proportion of Live cells was not substantially different from the control group after stretch for 12 and 24 h. After 6 and 12 h of cyclic stretch, there was no discernible difference in the rate of cell proliferation; however, after 24 h and 48 h, the cell proliferation rate increased by 27% and 52%, respectively. Apart from the mRNA expression of IL-8 and GROa was 1.41 times and 1.43 times higher than that of the control group in 9-hour groups, and RANTES mRNA expression was 1.38 times higher than that of the control group in 6-hour groups, there was also no appreciable difference in the expression levels of inflammatory factors such as IL1β, TNFα and PF4.
The Ligament cells became elongated and were rearranged after 12- and 24-hours' uniaxial stretch.

Conclusions Cyclic stretch encourages OPLL ligament cell proliferation and alteration of the cytoskeleton structure, but it has no effect on the inflammatory response or cell activity, which provides a new insight into the pathophysiology of OPLL.

†Tao Tang, Fuan Wang and Xizhe Liu contributed equally to this work.

*Correspondence:
Zhiyu Zhou
zhouzhy23@mail.sysu.edu.cn
Lin Chen
cltt107428@126.com

Full list of author information is available at the end of the article

Keywords OPLL, Mechanical stimulation, Cell proliferation, Cytoskeleton structure

Introduction

Ossification of the posterior longitudinal ligament (OPLL) is a common spinal condition characterized by ectopic ossification of the posterior longitudinal ligament [1, 2]. It frequently comes with severe compression of the spinal cord and nerve roots, which can manifest as quadriparesis or other myelopathy manifestations [3]. Although the cause of OPLL is unknown, numerous environmental and genetic variables are considered to be involved, which trigger ligament cells to differentiate into osteoblasts [4]. Spinal cord decompression is presently a well-established treatment option for those with advanced OPLL [5].

Mechanical stimulation (MS) is a type of physical force that has a variety of impacts on cells through regulating cell proliferation and differentiation [6]. It was demonstrated that chondrogenesis was induced by dynamic compression of the chondrocytes in polyglycolic acid [7]. In contrast to 15% mechanical stimulation, which had the opposite effects, 10% mechanical stimulation encourages the growth of vascular smooth muscle cells and suppresses apoptosis [8]. Our previous findings have shown that cyclic stretch promotes osteogenic differentiation of OPLL ligament cells (OPLL cells) [9, 10]. However, the effects of stretch stimulation on proliferation and viability of OPLL cells are yet unclear.

Mechanotransduction occurs when mechanical sensors withi'n cells interact with their surroundings, nearby cells, and a variety of cellular processes as part of a complicated and highly controlled system [11, 12]. Currently reported major mechanical sensors include the cell cytoskeleton, integrin-based focal adhesions, cell-cell junctions, ion channels, and the extracellular matrix [13–16]. When MS is applied to smooth muscle cells, the cytoskeletal architecture alters and the cells' actin filaments rearrange into stress fiber bundles in the same direction as the least stretch [17–19]. It is unclear, though, whether OPLL cells will exhibit comparable changes.

In this study, we investigated whether mechanical stimulation affected OPLL cells proliferation, morphology, viability, and inflammation by uniaxial cyclic stretching. We explored the response of mechanical stimulation to OPLL ligament cells during uniaxial cyclic stretch, which may shed light on the process of the pathological mechanism of OPLL.

Methods

Patients and ethics

Clinical history, physical examination, and computed tomography (CT) examinations were used to confirm the diagnosis of OPLL or non-OPLL (Figure S1). Specimens of the posterior longitudinal Ligament were obtained from patients during spinal surgery. 11 OPLL patients and 11 non-OPLL patients were selected for this study (Table 1). Each patient gave informed consent, and this study was authorized by the Seventh Affiliated Hospital of Sun Yat-sen University's ethics committee (Certificate No. 2020SYSUSH-055).

Cell culture

Posterior longitudinal ligament (PLL) specimens were collected during the anterior cervical decompression surgery. The ligament tissues were carefully removed from a non-ossified region to minimize contamination with osteogenic cells. PLL cells were extracted using the provided technique [20]. PLL tissues were thoroughly minced and digested for 4 h at 37 °C using 0.2% type II collagenase (Gibco). Then, at 5% CO2 and 37 °C, the digested tissues were plated into a T25 plate containing DMEM/F12 (Gibco) supplemented with 10% FBS (Gibco) and 1% penicillin/streptomycin (Gibco). Cells were digested using 0.25% trypsin-EDTA (Gibco) and then passed when confluent. Vimentin staining was used for cell type identification according to previous reports [21].

Cyclic stretch

We used a uniaxial cyclic stretch device to perform mechanical loading on the ligament cells, which was comparable to one previously described (Fig. 1A) [22]. OPLL cells was performed using previously published techniques with a few minor adjustments [23]. According to the instructions, 833μL of collagen I was fully mixed with 50mL of 20mM glacial acetic acid to form a Type I collagen/glacial acetic acid mixture of 50 μg/mL. In a nutshell, cells were seeded at a density of 1×10^4 cells/cm^2 on an elastic silicone membrane (Dow Corning, American) covered with 5 μg/cm^2 collagen I (Thermo Fisher Scientific, America, A1048301). Initially, cells were cultured in DMEM supplemented with 10% FBS. Then, the culture media were switched to 1% FBS DMEM for 24 h once the confluence had reached around 70%. After that, cells of test groups were exposed to 10% uniaxial cyclic stretch at frequency of 0.5 Hz for 3 h to 48 h at 37 °C in a humidified environment containing 5% CO_2.

RNA extraction and real-time quantitative polymerase chain reaction (RT–qPCR)

The RNAeasyTM Animal RNA Isolation Kit (Beyotime, China) was used to isolate total RNA, and the cDNA Synthesis Kit was used to turn 400 ng of total RNA into cDNA (TaKaRa, Japan). RT−qPCR was performed

Table 1 Tissue samples used in this study, including the clinical diagnosis, patient gender, age, and origin of each

OPLL				Non-OPLL			
Code	Type	Sex/age	Tissue	Code	Type	Sex/age	Tissue
1	Segmental	F/56	PLL	1	CDH	F/59	PLL
2	continuous	M/75	PLL	2	CDH	M/71	PLL
3	continuous	M/71	PLL	3	CSM	M/83	PLL
4	Mixed	F/59	PLL	4	CDH	M/59	PLL
5	Mixed	M/50	PLL	5	CDH	F/70	PLL
6	Segmental	F/53	PLL	6	CSM	F/57	PLL
7	Local	M/77	PLL	7	CDH	M/66	PLL
8	continuous	M/53	PLL	8	CDH	F/54	PLL
9	Segmental	M/53	PLL	9	CSM	M/66	PLL
10	Mixed	F/53	PLL	10	CDH	M/53	PLL
11	Segmental	F/59	PLL	11	CSM	M/58	PLL

OPLL Ossification of the posterior longitudinal ligament, *CDH* Cervical disc herniation, *CSM* Cervical spondylotic myelopathy, *PLL* Posterior longitudinal ligament

using qPCR Mix (Thermo Fisher Scientific, American) in a CXF-96 Real-Time System (Bio-Rad, American). Each reaction mixture contained 5μL of 2 PowerUpTM SYBRTM Green Master Mix, 2μL of nuclease-free water, 0.5μL of 10 mol/L forward and reverse primers, and 2μL of cDNA. The cycle conditions used were 2 min at 50 °C and 2 min at 95 °C, followed by 44 cycles of 15 s at 95 °C and 1 min at 60 °C.

Gene expression analysis

In this study, we examined the expression levels of specific genes—namely IL-1β, TNFα, IL-8, RANTES, GROα, and PF4—in OPLL Ligament cells subjected to cyclic stretch for 3, 6, and 9 h, using GAPDH as an endogenous control. The expression levels in Ligament cells prior to stretching served as the control group, and relative mRNA levels were analyzed using the $2^{-\Delta\Delta Ct}$ method. All primer sequences are provided in Table 2.

CCK8 assay and cytotoxicity test

We collected the extracts of stretch chamber at different time points to explore the cytotoxic effect of ligament cells. CCK8 assay was conducted using the CCK8 kit (Dojindo, China). Briefly, 1,000 cells were planted into each well with 100 μL medium, and 10 μL of CCK8 was added to each well. After incubation at 37 °C for 24 h in a humidified incubator with 5% CO_2, the proliferative ability of the cells was measured at 450 nm.

DMEM were stored respectively, which soaked in stretch chamber for 1, 3, and 7 days. PLL cells were cultured for collected DMEM and seeded at 30,000 cells/mL in a 96-well plate for 24 h. Cells were further cultured for 72 h, followed by Cell Counting Kit-8 (CCK-8) assay incubation for 4 h and absorbance measurement using a microplate reader.

Cell viability assay

Cell viability was assessed using calcein acetoxymethyl ester (calcein AM, eBioscience, Frankfurt, Germany) and propidium iodide (PI, MCE). In this system, green fluorescence indicates viable cells with intact membranes and red fluorescence indicates dead cells. After importing the images, ImageJ computed the number of green or red cells, accordingly. The PLL cells were incubated with a culture medium containing 1 μg/mL calcein AM and 1 μg/mL PI for 1 h at 37 °C. After washing with PBS, the cells were immediately viewed using fluorescence microscope (DM6B, Leica). The numbers of viable and dead cells were measured manually using ImageJ software.

Immunofluorescence staining

PLL cells were fixed in 4% paraformaldehyde for 20 min and washed 3 times with PBS. Sections were permeabilized and blocked in TBST (Biosharp, China) containing 0.3% Triton X-100 (Sigma, America) and 5% bovine serum albumin (BSA, BioFroxx, Germany). The samples were incubated with an anti-vimentin antibody (Abcam,1:100) overnight at 4 °C and goat anti-rabbit secondary antibody (Abcam, 1:300) for 1 h at room temperature. Nuclei were counterstained with 4,6-diamidino-2-phenylindole (DAPI, Abcam) for 5 min. Stains were visualized using a fluorescence microscope (Leica, Germany).

Phalloidin staining was performed to evaluate the impact of cyclic stretch on the cytoskeleton of OPLL cells. PLL cells were counterstained with phalloidin according to the manufacturer's instructions (MB5940, 1:100) in order to better observe the changes to the cytoskeleton. At last, nuclei were stained with DAPI. Images were acquired using a fluorescence microscope (DM6B, Leica).

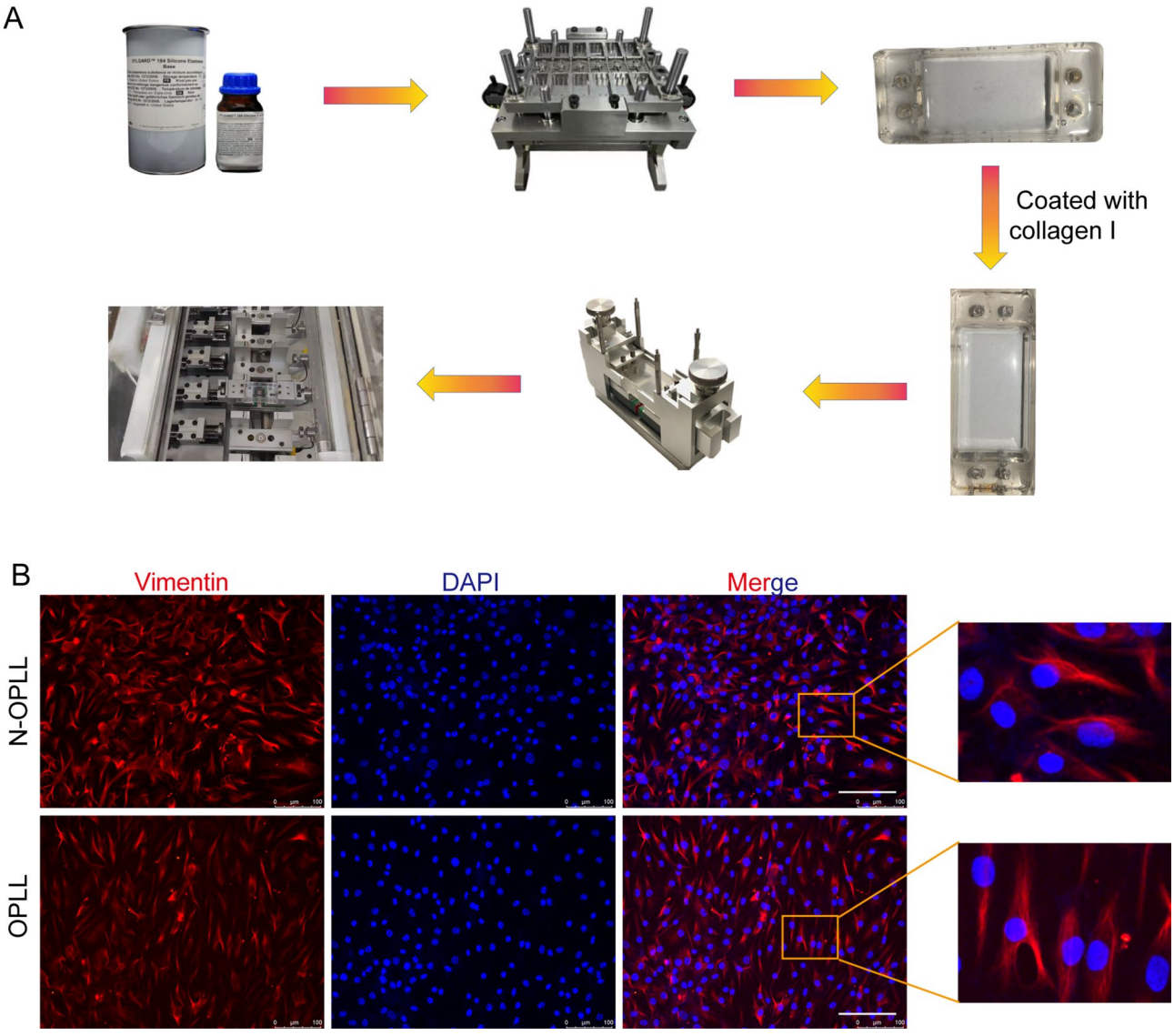

Fig. 1 **A** The process of stretch chamber and cells were cultured under dynamic stretch in the cyclic stretch apparatus. Referring to the SYLGARD™ 184 Silicone Elastomer material commonly used by domestic researchers for fabricating elastic stretch chamber, this material was processed using a custom-designed stainless-steel mold developed at our institution [23]. Subsequently, the bottom surface of the stretch chamber was coated with Type I collagen to enhance cell adhesion. Cells were then seeded into the chamber and subjected to dynamic mechanical stretching within a specialized mechanical stretching chamber. During this process, the cells adhered to the bottom of the stretch chamber were uniformly stretched. The magnitude and frequency of the stretching were precisely controlled by the mechanical stretching system. This system enables quantitative and uniform stretching of most cell types. It is equipped with a tension sensor, allows programmable control of stretch cycles, magnitude, and duration, and features real-time monitoring of CO_2 and O_2 concentrations. **B** Vimentin was visualized by immunofluorescence staining in spinal ligament cells. The scale bars = 20 μm, $n = 3$

Statistical analysis

SPSS version 20.0 (SPSS, USA) was used for statistical analysis. All values are provided as means standard deviation. The Shapiro-Wilk normality test was used to determine the normality of the data distribution. Statistical significance ($P \leq 0.05$) was determined using the student's *t*-test (two groups) or one-way analysis of variance (ANOVA) (more than two groups). For data with a non-normal distribution, the Mann-Whitney U test was used.

Results

Vimentin Immunofluorescence identified ligament cells as fibroblasts

In this study, Ligament cells were cultured at low density, exhibiting a mixed morphology of polygonal and spindle-shaped cells. Upon achieving a fusion rate of 70–80%, the cells predominantly assumed an elongated spindle shape with reduced translucent areas. Immunofluorescence staining of vimentin was used to determine the cell

Table 2 Primer sequences used in the study

Primer name	Sequence(5′→3′)
IL1β	Sense GTGGCAATGAGGATGACTTGTTCT
	Antisense TGTAGTGGTGGTCGGAGATTCG
TNFa	Sense CTTGTTCCTCAGCCTCTTCTCCTTC
	Antisense TTATCTCTCAGCTCCACGCCATTG
IL8	Sense CTCTCTTGGCAGCCTTCCTGATTT
	Antisense GGGTGGAAAGGTTTGGAGTATGTCT
RANTES	Sense TGCTGCTTTGCCTACATTGCC
	Antisense TCCTTGACCTGTGGACGACTGC
GROa	Sense CAGGGAATTCACCCCAAGAACA
	Antisense GGATGCAGGATTGAGGCAAGC
PF4	Sense GGTCCGTCCCAGGCACATC
	Antisense TCTTCAGCGTGGCTATCAGTTGG

Table 3 Effect of extracts on cell proliferation rate and toxicity grades

Group	RGR(%)	Grades
Control	100.00 ± 9.25	0
1d	96.46 ± 10.96	1
3d	91.56 ± 8.96	1
7d	86.42 ± 10.42	1

phenotype and the results showed that most of spinal ligament cells were fibroblasts (Fig. 1B).

Effect of stretch chamber extract on cytotoxicity

In order to explore the cytotoxic effect of Ligament cells, we collected the extracts of stretch chamber at different time points. The extract was added to 96-well plates seeded with Ligament cells and cultured for 72 h. The relative growth rates (RGR) of the 1-day, 3-day, and 7-day groups were 96.46 ± 10.96%, 91.56 ± 8.06%, and 86.42 ± 10.42%, respectively, and all groups of RGR were higher than 75% (Table 3). With the prolongation of immersion time in the stretch chamber, the cell proliferation rate decreased, but the difference was not statistically significant (Fig. 2, $p<0.05$).

Effect of Cyclic stretch on cell activity

To explore the influence of stretch on the cell vitality, we used the apparatus to submit ligament cells to cyclic stretch. The vitality of the OPLL cells was evaluated using calcein-AM/PI staining. The results showed that the cells

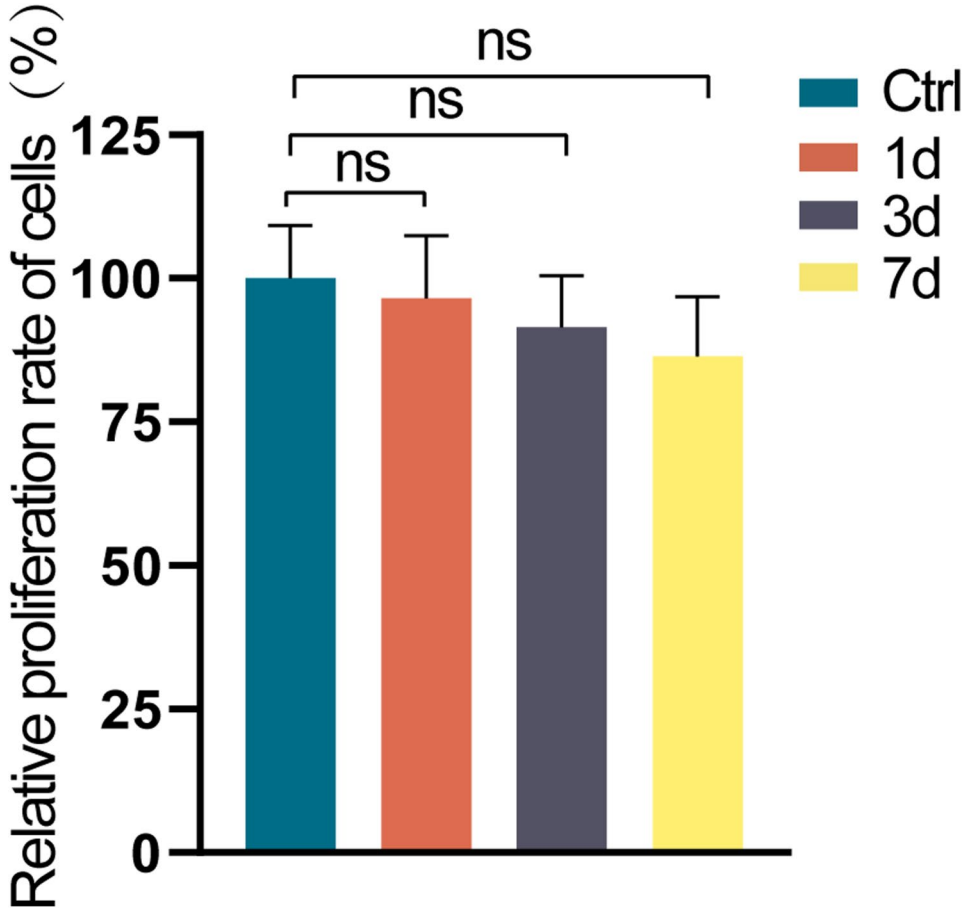

Fig. 2 Relative growth rate of PLL cells after co-culture with different groups of stretched chamber extracts. The stretched chambers were immersed in the DMEM medium for 1, 3, and 7 days to obtain extracts. Relative proliferation rate of cells cultured in the extracts for 72 h, $n=6$, one-way ANOVA analysis. *$p<0.05$, **$p<0.01$, ***$p<0.001$

survival rates in the static, 24-hour and 48-hour group were 79.52 ± 7.3%,84.62 ± 9.1% and 80.45 ± 6.9%, respectively and there was no significant difference among all groups (Fig. 3A and B, $p<0.05$). In addition, the results of cell activity were inconsistent with the results of the cell proliferation by CCK-8 assay.

Effect of Cyclic stretch on cell proliferation

To examine the effect of proliferation in OPLL cells, we measured the absorbance at 450 nm after 6 h, 12-hour, 24 h and 48 h of stretch by CCK-8 assay. The results showed that the cell proliferation rates of 6-hour group, 12-hour group, 24-hour group and 48-hour group were 109.12 ± 7.46%, 118.46 ± 12.86%, 127.46 ± 9.76%, 151.76 ± 12.14%, respectively. The findings revealed that the cell proliferation rate of the 6 h and the 12 h group did not change considerably (Fig. 4A and B, $p>0.05$)), while the cell proliferation rate of the 24 h and 48 h group increased by 27% and 52%, respectively in comparison to the static group (Fig. 4C and D, $p<0.05$).

The effect of Cyclic stretch on the production of Proinflammatory markers

We tested the production of inflammatory factors to confirm the effect of cyclic stretch on the release of proinflammatory indicators in OPLL cells. The results revealed that there was no significant difference in IL1β, TNFα and PF4 levels between the two groups (Fig. 5A, B and F, $p>0.05$). Additionally, there was no discernible variation in the expression levels of inflammatory factors at other

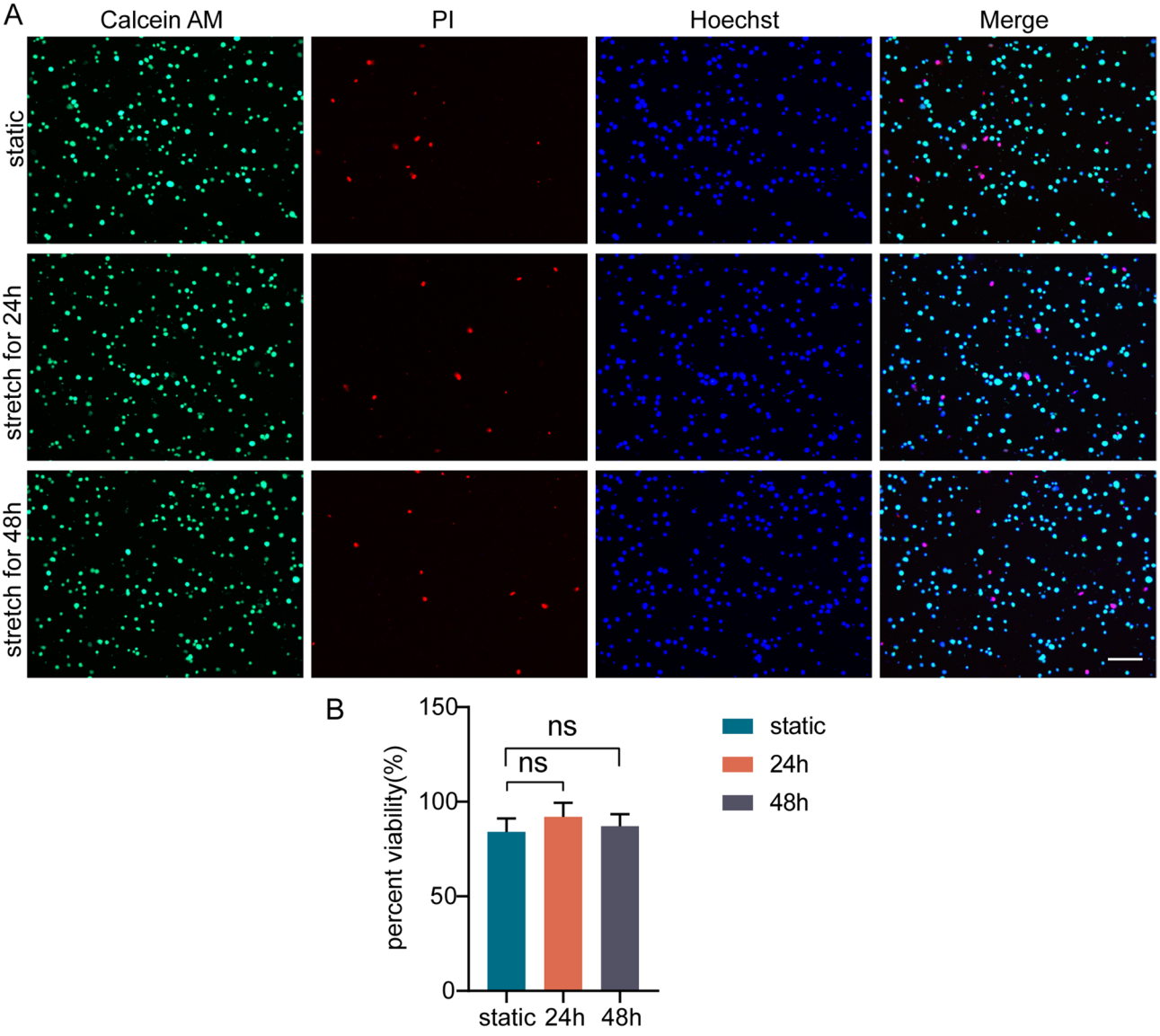

Fig. 3 Typical fluorescence microscope showing the dead cells (red) and viable cells (green) after cyclic stretch at different time points (0 h, 24 h, and 48 h). Scale bars, 200 μm, $n=3$, one-way ANOVA analysis. * $p<0.05$, ** $p<0.01$, *** $p<0.001$

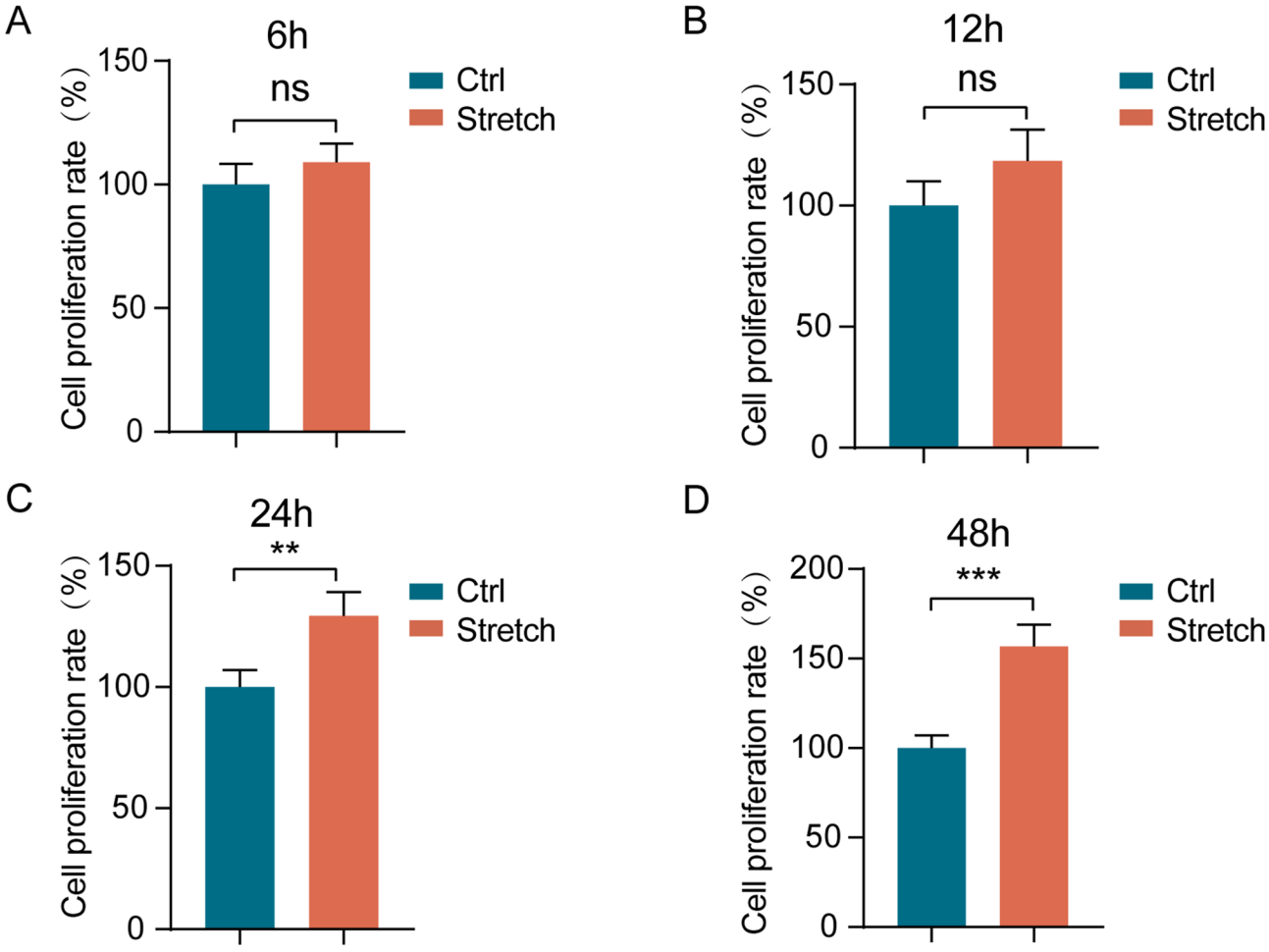

Fig. 4 Effect of cyclic stretch on OPLL cells growth. **A** The relative growth rate of cells stretched repeatedly for 6 h, $n=3$. **B** The relative growth rate of cells stretched repeatedly for 12 h, $n=3$. **C** The relative growth rate of cells that were stretched cyclically for 24 h, $n=3$. **D** The relative growth rate of cells that have been stretched cyclically for 48 h. $n=3$, two-tailed student's *t*-test. * $p<0.05$, ** $p<0.01$, *** $p<0.001$

time periods ($p>0.05$), with the exception of IL8 and GROa in 9 hours' group and RANTES in 6 hours' group (Fig. 5C and E, $p<0.05$).

Effect of Cyclic stretch on the cytoskeletal structure

To evaluate the impact of cyclic stretch on the cytoskeleton of OPLL cells, phalloidin staining was performed. Without cyclic stretch stimulation, OPLL cells were fusiform, flat, or polygonal in shape. Following stimulation for 12 h, the cells' anteroposterior diameter increased, which was consistent with the direction of stretch. Following a 24-hour stretch, the cytoskeleton was reorganized and the anteroposterior diameters were significantly stretched (Fig. 6A). The results of semi-quantitative analysis showed that the cell length/width ratio in static group, 12-hour group and 24-hour group was 3.57 ± 0.51,6.73 ± 0.62 and 9.65 ± 0.87, respectively, and the difference was statistically significant (Fig. 6B, $p<0.05$).

Discussion

OPLL is a common spinal condition characterized by ectopic bone development in the posterior longitudinal ligament, and its cause is unknown [24]. There is growing evidence that mechanical stimulation plays a significant role in the evolution of OPLL, however, the response of mechanical stimulation to OPLL remains unknown during this process [20, 25–27]. In this study, OPLL cells are stimulated in the uniaxial cyclic stretch apparatus. These results suggested that mechanical stimulation promotes OPLL cells proliferation and cytoskeleton remodeling, but not inflammatory response and cell viability.

New mechanobiological phenomena, such cell proliferation, differentiation, and inflammatory response, are made visible by in vitro stretch stimulation [28]. It was reported that the rate of fibroblasts proliferation remains low in dilute collagen gels, with only a (14 ± 7) % increase in cell number from day 3 to day 7 in static culture. When fibroblasts were cultivated under dynamic circumstances, they were shown to immediately re-enter the cell cycle

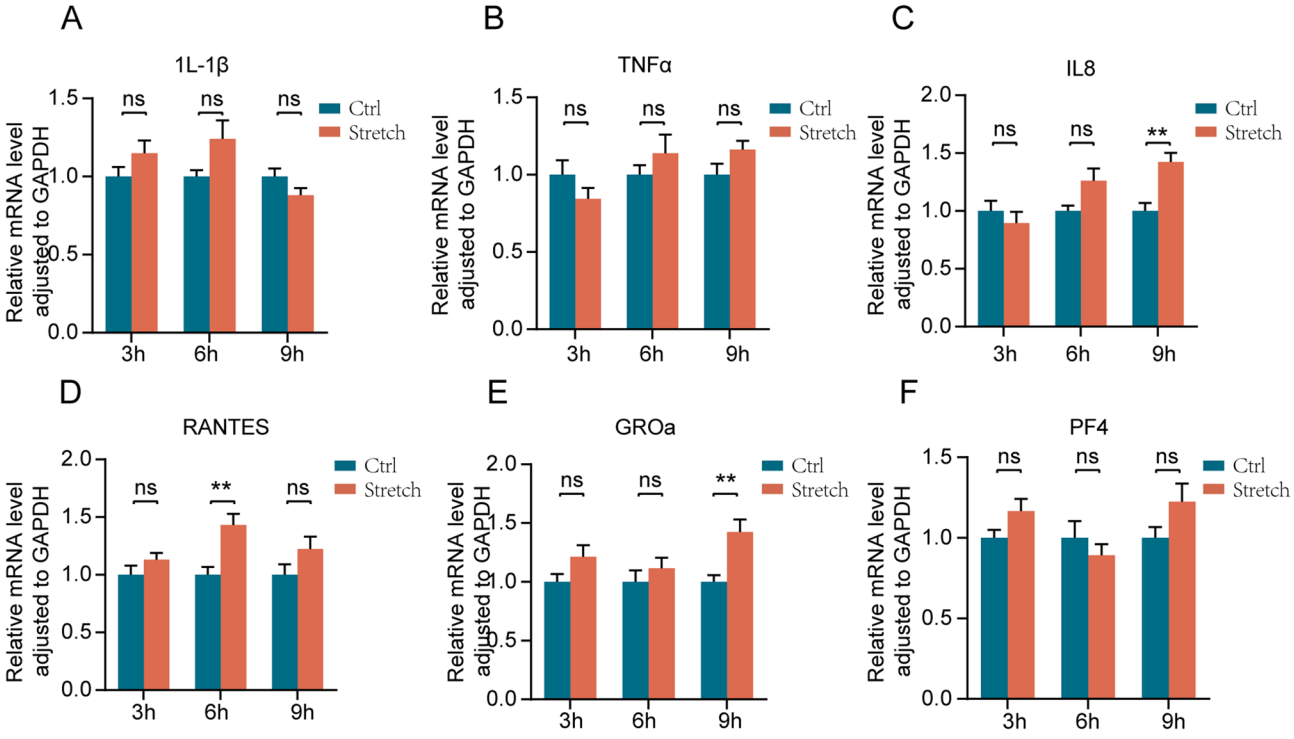

Fig. 5 The effect of uniaxial cyclic stretch on inflammation-related gene production in OPLL ligament cells. **A**-**F** It depicts a comparison of the expression of inflammatory factors IL1, TNFα, IL8, RANTES, GROa, and PF4 in cells from the static and stretch groups. Data are shown as the mean standard deviation of the average change fold of inflammatory gene expression in the experimental group relative to the control group, $n=3$, two-tailed student's *t*-test. * $p<0.05$, ** $p<0.01$, *** $p<0.001$

and begin dividing [29]. Besides, previous studies have shown that fluid shear stress cannot inhibit fibroblasts proliferation, while, cyclic stretch was a key biophysical element in fibroblast growth [30, 31]. The proliferation rate did not change considerably after 6 h and 12 h of stretch, but rose significantly after 24 h and 48 h of stretch, according to this study. These results indicate that prolonged cyclic stretch promote the proliferation of OPLL cells and cyclic stretch did not affect the viability of OPLL cells. We believe that cells must have a particular reaction time after stretching to re-enter the cell cycle, and that cells stimulated by a shorter stretch time are unable to transform mechanical signal into intracellular chemical signals, which affects the intracellular mitotic stage. The frequency and amplitude also have an impact on cell growth. Future research will examine the impact of other stretch amplitudes and frequencies on cell growth [32, 33].

It has also been proposed that the inflammatory response, whose activation is triggered by cellular environmental stimuli, plays a significant role in the ossification of spinal ligaments. According to recent research, fibroblasts may actively participate in the control of inflammatory reactions following mechanical stimulation [34–36]. After mechanical stretch, fibroblasts that were identified and cultivated during the cystic stage of lung formation may be a significant source of cytokines that promote inflammation [37]. It has been shown that mechanical stretch involved in the NF-κB signaling pathway in OPLL cells [38]. The protein level of p-p65 was dramatically increased in Ligament cells after 15–30 min of stimulation and inflammatory cytokines such as Il-1, IL-6, and TNFα were considerably elevated in spinal Ligament cells after 24 h of stress [39]. However, our findings demonstrated that OPLL cells did not significantly respond to stretch by activating the transcription of inflammatory factors. We concluded that short-term stretch did not significantly trigger the transcription of inflammatory factors except for the increased expression of some factors. We believe that the stretch time is brief and that the inflammatory response has not yet been started. To further examine the association between mechanical stimulation and inflammatory response in OPLL cells, we will need to increase the sample size and length of time in the future.

The cytoskeleton is a network of actin filaments, microtubules, and intermediate filaments that serve as mechanical links between different regions of the cell and connect the cell membrane to the nucleus [40, 41]. Integrin receptors bridge the gap between the cytoskeleton and the extracellular matrix via the plasma membrane [42, 43]. The mechanical stimulation placed on

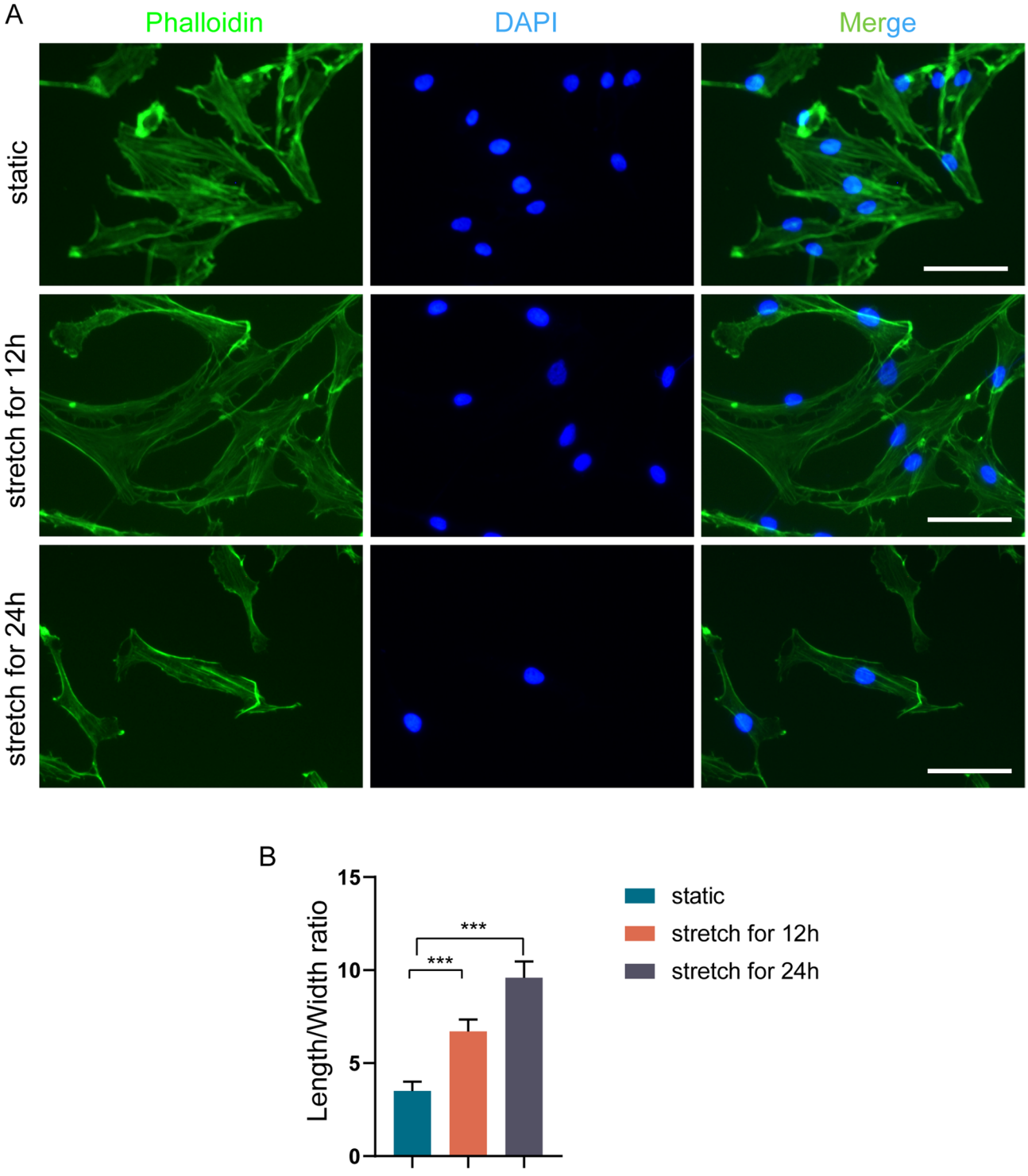

Fig. 6 Phalloidin was used to stain the F-actin cytoskeleton of the OPLL cells in several groups. **A** The cytoskeletal organization was altered and the anteroposterior diameter of the OPLL cells dramatically increased after 12 and 24 h of stretch, respectively, **B** The cell length/width ratio of different groups was determined by the semi-quantitative analysis of phalloidin staining, scale bar = 20 μm, $n = 3$, one-way ANOVA analysis. * $p<0.05$, ** $p<0.01$, *** $p<0.001$

the extracellular matrix can therefore be transmitted to the cytoskeleton [44, 45]. Integrin receptors have been linked to mechanical stimulation-induced cell deformation and secondary cytoskeleton tension, and mechanical stimulation of the cytoskeleton can be paired with chemical processes during mechanochemical transmission [46–48]. Cytoskeletal remodeling and mechanochemical transduction can affect cell proliferation, differentiation

and migration [49, 50]. In this study, we found that the morphological changes of the cells were slightly longer after 12 h of stretch by phalloidin staining. After stimulation for 24 h, their anteroposterior diameter greatly increased, the cytoskeletal organization was altered, and the static cells had a flattened appearance. Thus, cyclic stretch leads to cell elongation and actin cytoskeleton remodeling. These results indicated that stretch stimulation induced actin cytoskeleton remodeling in OPLL ligament cells.

Understanding possible alterations in mechanobiological features that contribute to disease pathology through mechanical stimulation is crucial [51]. Many laboratories have independently produced uniaxial cyclic stretching devices, which have been used to explore mechanobiology [52–54]. Some of these devices are commercially accessible, such as Flexcell, Strex, Electron Microscope Sciences, etc [55–60]. With the exception of a few cutting-edge devices, such as the commercial Flexcell system, which mainly rely on intricate pneumatic control systems to manage air pressure, the majority of these devices have considerable limits, and most instrument fine tuning has not been proved [61]. In order to identify the activation of cellular stretch-signaling molecular machinery, we created a non-toxic, transparent, elastic stretched chamber that is advantageous to cell adhesion development and can tolerate repeated exposure to high temperatures. In addition, the apparatus also has a tension sensor that allows for free setting of stretching periods, amplitude, and time as well as real-time monitoring of oxygen and carbon dioxide concentrations and hypoxic culture. According to our findings, we concluded there was no evident cytotoxicity in stretch chamber. The creation and improvement of the dynamic stretch culture system provides technological assistance and execution strategies for future studies of the OPLL molecular mechanism.

This study has some limitations that should be noted. First, due to sample size constraints, we were unable to distinguish the illness categories into segmental, continuous, mixed, and localized OPLL in this study, and a bigger sample scale is required to support our results. Second, due to the function of the custom-made uniaxial stretch apparatus, only sinusoidal stretching mode was possible. As a result, the cells had no rest throughout the stretching process, which may be inconsistent with normal cervical physiological activity. Third, although we discovered that uniaxial cyclic stretch increased morphological alterations and proliferation in OPLL cells, the detailed mechanism by which it occurs remains obscure. Finally, the experiment was only carried out in vitro since it was challenging to create an animal model of local heterotopic ossification of the PLL brought on by mechanical stimulation.

Conclusions

In this work, uniaxial cyclic stretch encourages OPLL cells proliferation but has no impact on inflammatory response or cell activity. Cytoskeletal structures change in response to cyclical stretch stimulation. Furthermore, this discovery provides operational and technological strategies for more research into the OPLL molecular mechanism.

Supplementary Information

The online version contains supplementary material available at https://doi.org/10.1186/s12891-025-09142-5.

Supplementary Material 1.

Acknowledgements

Not applicable.

Authors' contributions

T T and FA W: conceptualization, investigation, writing original draft. XZ L: methodology, figures preparation and data analysis. SY L: funding acquisition. ZY Z: conceptualization, supervision, editing, and provided funding support. L C: conceptualization, supervision, project administration and funding support. All authors have read and agreed to the published version of the manuscript.

Funding

the National Natural Science Foundation of China (U22A20162,31900583, 32071351, 81772400,82102604, 81960395), foundation of Shenzhen Committee for Science and Technology Innovation(JCYJ20190809142211354), Sanming Project of Medicine in Shenzhen (SZSM201911002), the Beijing Municipal Health Commission (Grant No. BMHC-2021-6, BMHC-2019-9, BMHC-2018-4, PXM2020_026275_000002), AO CMF CPP on Bone Regeneration (AOCMF-21–04 S, supported by AO Foundation, AO CMF. AO CMF is a clinical division of the AO Foundation - an independent medically-guided not-for-profit organization), Sun Yat-sen University Clinical Research 5010 Program (2019009).

Data availability

The data that support the findings of this study are available from the authors but restrictions apply to the availability of these data, which were used under license from the Seventh Affiliated Hospital of Sun Yat-sen University's ethics committee for the current study, and so are not publicly available. Data are, however, available from the authors upon reasonable request and with permission from the Seventh Affiliated Hospital of Sun Yat-sen University's ethics committee.

Declarations

Ethics approval and consent to participate

This study was approved by the Ethics Committee of the Seventh Affiliated Hospital of Sun Yat-sen University (Certificate No. 2020SYSUSH-055), and informed consent was obtained from each patient. The processing of clinical tissue samples was in strict compliance with the ethical standards of the Declaration of Helsinki. All patients that participated in this study signed a written informed consent.

Consent for publication

Consent for publication was obtained from all the participants.

Competing interests

The authors declare no competing interests.

Author details

[1]Department of Orthopedic Surgery, The Second Affiliated Hospital of Anhui Medical University, Hefei, Anhui, China

[2]Innovation Platform of Regeneration and Repair of Spinal Cord and Nerve injury, Department of Orthopaedic Surgery, The Seventh Affiliated Hospital, Sun Yat-sen University, Shenzhen 518107, China
[3]Guangdong Provincial Key Laboratory of Orthopedics and Traumatology, The First Affiliated Hospital of Sun Yat-sen University, Guangzhou, China
[4]Department of Ophthalmology, The Second Affiliated Hospital of Anhui Medical University, Hefei, Hefei 230000, China

Received: 6 April 2024 / Accepted: 20 August 2025
Published online: 30 September 2025

References

1. Matsunaga S, Sakou T. Ossification of the posterior longitudinal ligament of the cervical spine: etiology and natural history. Spine (Phila Pa 1976). 2012;37(5):E309-14.
2. Terayama K. Genetic studies on ossification of the posterior longitudinal ligament of the spine. Spine (Phila Pa 1976). 1989;14(11):1184–91.
3. Xu C, et al. The microRNA-10a/ID3/RUNX2 axis modulates the development of ossification of posterior longitudinal ligament. Sci Rep. 2018;8(1): 9225.
4. Kimura A, et al. Impact of diabetes mellitus on cervical spine surgery for ossification of the posterior longitudinal ligament. J Clin Med. 2021. https://doi.org/10.3390/jcm10153375.
5. Boody BS, Lendner M, Vaccaro AR. Ossification of the posterior longitudinal ligament in the cervical spine: a review. Int Orthop. 2019;43(4):797–805.
6. Cho H, Park HJ, Seo YK. Induction of *PLXNA4* gene during neural differentiation in human umbilical-cord-derived mesenchymal stem cells by low-intensity sub-sonic vibration. Int J Mol Sci. 2022. https://doi.org/10.3390/ijms23031522.
7. Shadi M, et al. Optimizing artificial meniscus by mechanical stimulation of the chondrocyte-laden acellular meniscus using ad hoc bioreactor. Stem Cell Res Ther. 2022;13(1): 382.
8. Wang X, et al. Yes-associated protein reacts differently in vascular smooth muscle cells under different intensities of mechanical stretch. Aging. 2022;14(1):286–96.
9. Zhu Z, et al. Uniaxial Cyclic stretch enhances osteogenic differentiation of OPLL-derived primary cells via YAP-Wnt/beta-catenin axis. Eur Cell Mater. 2023;45:31–45.
10. Tang T, et al. DLX5 regulates the osteogenic differentiation of spinal ligaments cells derived from ossification of the posterior longitudinal ligament patients via NOTCH signaling. JOR Spine. 2023;6(2): e1247.
11. Lappalainen P, et al. Biochemical and mechanical regulation of actin dynamics. Nat Rev Mol Cell Biol. 2022;23(12):836–52.
12. De Belly H, et al. Membrane tension gates ERK-Mediated regulation of pluripotent cell fate. Cell Stem Cell. 2021;28(2):273–84. .e6.
13. Mylvaganam S, et al. The spectrin cytoskeleton integrates endothelial mechanoresponses. Nat Cell Biol. 2022;24(8):1226–38.
14. Reyes Fernandez PC, et al. Gabapentin disrupts binding of Perlecan to the α(2)δ(1) voltage sensitive calcium channel subunit and impairs skeletal mechanosensation. Biomolecules. 2022. https://doi.org/10.3390/biom12121857.
15. Li CW, et al. Mechanically induced formation and maturation of 3D-matrix adhesions (3DMAs) in human mesenchymal stem cells. Biomaterials. 2020;258: 120292.
16. Wang L, et al. Mechanical sensing protein PIEZO1 regulates bone homeostasis via osteoblast-osteoclast crosstalk. Nat Commun. 2020;11(1): 282.
17. Wan F, et al. Hydroxyapatite-reinforced alginate fibers with bioinspired dually aligned architectures. Carbohydr Polym. 2021;267:118167.
18. Redondo A, et al. Melt-spun nanocomposite fibers reinforced with aligned tunicate nanocrystals. Polymers. 2019. https://doi.org/10.3390/polym11121912.
19. Sugita S, et al. Stress fibers of the aortic smooth muscle cells in tissues do not align with the principal strain direction during intraluminal pressurization. Biomech Model Mechanobiol. 2021;20(3):1003–11.
20. Chen S, et al. Combined use of leptin and mechanical stress has osteogenic effects on ossification of the posterior longitudinal ligament. Eur Spine J. 2018;27(8):1757–66.
21. Yang HS, et al. Mechanical strain induces Cx43 expression in spinal ligament fibroblasts derived from patients presenting ossification of the posterior longitudinal ligament. Eur Spine J. 2011;20(9):1459–65.
22. Yu L, et al. Biomimetic bone regeneration using angle-ply collagen membrane-supported cell sheets subjected to mechanical conditioning. Acta Biomater. 2020;112:75–86.
23. Li JM, et al. Uniaxial cyclic stretch promotes osteogenic differentiation and synthesis of BMP2 in the C3H10T1/2 cells with BMP2 gene variant of rs2273073 (T/G). PLoS One. 2014;9(9): e106598.
24. Bernstein DN, et al. National trends and complications in the surgical management of ossification of the posterior longitudinal ligament (OPLL). Spine (Phila Pa 1976). 2019;44(22):1550–7.
25. Xu C, et al. Small extracellular vesicle-mediated miR-320e transmission promotes osteogenesis in OPLL by targeting TAK1. Nat Commun. 2022;13(1):2467.https://doi.org/10.1038/s41467-022-29029-6
26. Tokuhashi Y, Ajiro Y, Umezawa N. A patient with two re-surgeries for delayed myelopathy due to progression of ossification of the posterior longitudinal ligaments after cervical laminoplasty. Spine (Phila Pa 1976). 2009;34(2):E101-5.
27. Chen D, et al. Role of Cx43-Mediated NFsmall ka, CyrillicB signaling pathway in ossification of posterior longitudinal ligament: an in vivo and in vitro study. Spine (Phila Pa 1976). 2017;42(23):pE1334–E1341.
28. Yu JH, et al. Bile acids promote gastric intestinal metaplasia by upregulating CDX2 and MUC2 expression via the FXR/NF-κB signalling pathway. Int J Oncol. 2019;54(3):879–92.
29. Wahlsten A, et al. Mechanical stimulation induces rapid fibroblast proliferation and accelerates the early maturation of human skin substitutes. Biomaterials. 2021;273:120779.
30. Elashry MI, et al. Influence of mechanical fluid shear stress on the osteogenic differentiation protocols for equine adipose tissue-derived mesenchymal stem cells. Acta Histochem. 2019;121(3):344–53.
31. Zhang L, et al. Mechanical stress regulates osteogenic differentiation and RANKL/OPG ratio in periodontal ligament stem cells by the Wnt/β-catenin pathway. Biochim Biophys Acta. 2016;1860(10):2211–2219.
32. Chen D, et al. Connexin 43 promotes ossification of the posterior longitudinal ligament through activation of the ERK1/2 and p38 MAPK pathways. Cell Tissue Res. 2016;363(3):765–73.
33. Tanno M, et al. Uniaxial cyclic stretch induces osteogenic differentiation and synthesis of bone morphogenetic proteins of spinal ligament cells derived from patients with ossification of the posterior longitudinal ligaments. Bone. 2003;33(4):475–84.
34. Le Bellego F, et al. Mechanical strain increases cytokine and chemokine production in bronchial fibroblasts from asthmatic patients. Allergy. 2009;64(1):32–9.
35. Kunanusornchai W, Muanprasat C, Chatsudthipong V. Adenosine monophosphate-activated protein kinase activation and suppression of inflammatory response by cell stretching in rabbit synovial fibroblasts. Mol Cell Biochem. 2016;423(1–2):175–85.
36. Jiang C, et al. Repetitive mechanical stretching modulates transforming growth factor-β induced collagen synthesis and apoptosis in human patellar tendon fibroblasts. Biochem Cell Biol. 2012;90(5):667–74.
37. Hawwa RL, et al. IL-10 inhibits inflammatory cytokines released by fetal mouse lung fibroblasts exposed to mechanical stretch. Pediatr Pulmonol. 2011;46(7):640–9.
38. Aung KH, et al. Glabridin attenuates the retinal degeneration induced by sodium iodate in vitro and in vivo. Front Pharmacol. 2020;11: 566699.
39. Shi L, et al. Endoplasmic reticulum stress regulates mechanical stress-induced ossification of posterior longitudinal ligament. Eur Spine J. 2019;28(10):2249–56.
40. Usukura E, et al. An unroofing method to observe the cytoskeleton directly at molecular resolution using atomic force microscopy. Sci Rep. 2016;6: 27472.
41. Li X, et al. Rhein derivative 4F inhibits the malignant phenotype of breast cancer by downregulating Rac1 protein. Front Pharmacol. 2020;11: 754.
42. Knorr S, et al. Identification and characterization of immunodominant proteins from tick tissue extracts inducing a protective immune response against *Ixodes ricinus* in cattle. Vaccines. 2021;9(6): 636.
43. Xi K, et al. Microenvironment-responsive immunoregulatory electrospun fibers for promoting nerve function recovery. Nat Commun. 2020;11(1): 4504.
44. Dastani K, et al. Effect of input voltage frequency on the distribution of electrical stresses on the cell surface based on single-cell dielectrophoresis analysis. Sci Rep. 2020;10(1): 68.
45. Yang D, et al. Analysis of factors limiting bacterial growth in PDMS mother machine devices. Front Microbiol. 2018;9: 871.
46. Byron A, et al. Characterisation of a nucleo-adhesome. Nat Commun. 2022;13(1): 3053.

47. Lluis F, et al. Periodic activation of Wnt/beta-catenin signaling enhances somatic cell reprogramming mediated by cell fusion. Cell Stem Cell. 2008;3(5):493–507.
48. Weber LM, et al. The effects of cell-matrix interactions on encapsulated beta-cell function within hydrogels functionalized with matrix-derived adhesive peptides. Biomaterials. 2007;28(19):3004–11.
49. Manshian BB, et al. High-content imaging and gene expression approaches to unravel the effect of surface functionality on cellular interactions of silver nanoparticles. ACS Nano. 2015;9(10):10431–44.
50. Wang A, et al. Fast stiffness mapping of cells using high-bandwidth atomic force microscopy. ACS Nano. 2016;10(1):257–64.
51. Li D, et al. Astigmatic traction force microscopy (aTFM). Nat Commun. 2021;12(1): 2168.
52. Richard MN, et al. Mechanical stretching stimulates smooth muscle cell growth, nuclear protein import, and nuclear pore expression through mitogen-activated protein kinase activation. J Biol Chem. 2007;282(32):23081–8.
53. Matsugaki A, Fujiwara N, Nakano T. Continuous cyclic stretch induces osteoblast alignment and formation of anisotropic collagen fiber matrix. Acta Biomater. 2013;9(7):7227–35.
54. O'Callaghan CJ, Williams B. Mechanical strain-induced extracellular matrix production by human vascular smooth muscle cells: role of TGF-beta(1). Hypertension. 2000;36(3):319–24.
55. Roth KB, et al. Imaging of a linear diode bar for an optical cell stretcher. Biomed Opt Express. 2015;6(3):807–14.
56. Mayer CR, et al. Characterization of 3D printed stretching devices for imaging force transmission in Live-Cells. Cell Mol Bioeng. 2019;12(4):289–300.
57. Huang L, Mathieu PS, Helmke BP. A stretching device for high-resolution live-cell imaging. Ann Biomed Eng. 2010;38(5):1728–40.
58. Huang Y, Nguyen NT. A polymeric cell stretching device for real-time imaging with optical microscopy. Biomed Microdevices. 2013;15(6):1043–54.
59. Daulagala AC, et al. A simple method to test mechanical strain on epithelial cell monolayers using a 3D-Printed stretcher. Methods Mol Biol. 2021;2367:235–47.
60. Boulter E, et al. Cyclic uniaxial mechanical stretching of cells using a LEGO(®) parts-based mechanical stretcher system. J Cell Sci. 2020. https://doi.org/10.1242/jcs.234666.
61. Ning SL, et al. Genetic differences in osteogenic differentiation potency in the thoracic ossification of the ligamentum flavum under cyclic mechanical stress. Int J Mol Med. 2017;39(1):135–43.

Publisher's Note